

## Research Article

# Potential Therapeutic Role of Hispidulin in Gastric Cancer through Induction of Apoptosis via NAG-1 Signaling

Chao Yuan Yu,<sup>1</sup> Kang-Yi Su,<sup>2,3</sup> Po-Lei Lee,<sup>4</sup> Jie-Yu Jhan,<sup>1</sup> Po-Hung Tsao,<sup>1</sup> De-Chuan Chan,<sup>5</sup> and Yi-Lin Sophia Chen<sup>1</sup>

<sup>1</sup> Department of Biotechnology and Animal Science, College of Bioresources, National Ilan University, Ilan 260, Taiwan

<sup>2</sup> Department of Clinical Laboratory Sciences and Medical Biotechnology, College of Medicine, National Taiwan University, Taipei 100, Taiwan

<sup>3</sup> Department of Laboratory Medicine, National Taiwan University Hospital, Taipei 100, Taiwan

<sup>4</sup> Department of Electrical Engineering, National Central University, Zhongli 32001, Taiwan

<sup>5</sup> Division of General Surgery, Department of Surgery, Tri-Service General Hospital, Taipei 114, Taiwan

Correspondence should be addressed to Yi-Lin Sophia Chen; a221865880@yahoo.com.tw

Received 12 March 2013; Revised 7 June 2013; Accepted 9 June 2013

Academic Editor: Thomas Efferth

Copyright © 2013 Chao Yuan Yu et al. This is an open access article distributed under the Creative Commons Attribution License, which permits unrestricted use, distribution, and reproduction in any medium, provided the original work is properly cited.

Gastric cancer is one of the most common malignant cancers due to poor prognoses and high mortality rates worldwide. However, an effective chemotherapeutic drug without side effects remains lacking. *Saussurea involucreata* (SI) Kar. et Kir., also known as snow lotus, grows in mountainous rocky habitats at 2600 m elevation in the Tian Shan and Aer Tai regions of China. The ethyl acetate extract of SI had been shown to inhibit proliferation and induce apoptosis in various tumor cells. In this study, we demonstrated that Hispidulin, active ingredients in SI, inhibits the growth of AGS gastric cancer cells. After Hispidulin treatment, NAG-1 remained highly expressed, whereas COX-2 expression was downregulated. Flow cytometric analysis indicated that Hispidulin induces G1/S phase arrest and apoptosis in time- and concentration-dependent manners. G1/S arrest correlated with upregulated p21/WAF1 and p16 and downregulated cyclin D1 and cyclin E, independent of p53 pathway. In addition, Hispidulin can elevate Egr-1 expression and ERK1/2 activity, whereas ERK1/2 inhibitor markedly attenuated NAG-1 mediated apoptosis. Taken together, Hispidulin can efficiently activate ERK1/2 signaling followed by NAG-1 constitutive expression and trigger cell cycle arrest as well as apoptosis in cancer cell. It can be a potential compound for combination therapy of gastric cancer in the future.

## 1. Introduction

Gastric cancer is one of the most common causes of cancer-related mortality in China and other Asian countries [1, 2]. Surgery and chemotherapy are the standard treatment modalities for gastric cancer [3–5]. The 5-year survival of gastric cancer patients is currently estimated at approximately 30%; therefore, the development of novel treatment strategies to improve patients' prognoses is urgently required. The majority of gastric adenocarcinomas express high levels of cyclooxygenase-2 (COX-2) [6–9]. Houghton et al. reported that angiogenesis and *Helicobacter pylori* infection are both associated with COX-2 expression in gastric cancer patients

[10]. The knockdown of COX-2 in a SGC-7901 gastric adenocarcinoma cell line by RNA interference inhibited proliferation and induced apoptosis, indicating that suppression of COX-2 might represent an effective approach for the treatment of gastric cancer. The majority of selective COX-2 inhibitors exert pronounced side effects that limit their administration. Based on this clinical phenomena, AGS gastric adenocarcinoma cell line which constitutively expressed both COX-1 and COX-2 and additional COX-2 induced by IL-1 $\beta$  to potentially make it an excellent model for assessing gastrointestinal toxicity of COX-2 inhibitors was an ideal model to evaluate the potential compound for adjuvant therapy in gastric cancer [11]. In this study, we observed that

Hispidulin inhibited the proliferation of AGS gastric adenocarcinoma cells; therefore, we aimed to establish if the mechanism underlying the antiproliferative effects of Hispidulin on AGS cells is the downregulation of COX-2 expression.

In our previous study, isochaihulactone markedly upregulated the expression of the nonsteroidal anti-inflammatory-drug- (NSAID-) activated gene-1 (*NAG-1*; also known as *MIC-1*, *GDF-15*, placental *TGF- $\beta$* , and *PLAB*). *NAG-1* is a transforming growth factor- $\beta$ -like secreted protein, initially characterized as a p53-regulated gene [12–14]. Overexpression of *NAG-1* in breast cancer cells resulted in growth arrest and apoptosis *in vitro* and *in vivo*. Previous studies observed similar results in colon cancer cells [15–17] and following the treatment of prostate cancer cells with purified *NAG-1* [18]. These findings suggested that *NAG-1* is associated with apoptosis and that the downregulation of *NAG-1* expression might promote tumorigenesis. In our previous investigation, we identified that isochaihulactone, a novel lignan isolated from the root of *Bupleurum scorzonerifolium*, induced microtubule depolymerization, cell cycle arrest, and proapoptotic activity in A549 human lung cancer cells [19]. We also observed that NSAIDs upregulated the expression of several isochaihulactone-induced genes and that isochaihulactone upregulated *NAG-1* protein expression in a time-dependent manner. The upregulation of *NAG-1* by isochaihulactone was associated with the upregulation of *EGR-1* expression; therefore, the silencing of *EGR-1* expression by siRNAs could also be associated with downregulated *NAG-1* RNA and protein expression. In our analyses, the MEK1/2 inhibitor PD98059 reduced the inhibitory effects of isochaihulactone significantly; however, the p38 inhibitor SB203580 and the JNK inhibitor SP600125 did not limit isochaihulactone-induced growth inhibition. The MEK1/2 inhibitor PD98059 reduced isochaihulactone-induced upregulation of *EGR-1* and *NAG-1* protein expression, whereas SB203580 and SP600125 had nonsignificant effects on *EGR-1* and *NAG-1* expression. These data supported the concept that isochaihulactone-induced ERK1/2 activity is critical for the regulation of *EGR-1* and *NAG-1* expression. The induction of ERK1/2 activity and subsequent induction of *EGR-1* and *NAG-1* contributes to the growth inhibitory and apoptosis-promoting effects of antitumor compounds in cancer cells.

*Saussurea involucreata* Kar. et Kir., or the snow lotus, grows in mountainous rocky habitats at 2600 m elevation or higher in the Tian Shan and Aër Tai regions of China. Because of excessive harvesting of the wild plants for use in pharmaceutical preparations and their remarkably slow growth, the wild population of *S. involucreata* has depleted in recent years. *S. involucreata* is currently close to extinction and, therefore, listed as a second-grade national protected wild plant in China [20, 21]. According to the theories of traditional Chinese medicine, *S. involucreata* has the effects of warming the kidney, activating “yang,” expelling wind, eliminating dampness, inducing menstruation, and promoting blood circulation [22]. Hispidulin (40,5,7-trihydroxy-6-methoxyflavone) is a naturally occurring flavone in *S. involucreata* [20]. Several studies have shown its potent antioxidative, antifungal, anti-inflammatory, antimutagenic, and antineoplastic properties *in vitro* [23–25]. A recent study identified Hispidulin as a

potent ligand of the human central benzodiazepine receptor *in vitro* [26]. Hispidulin also acts as a partial positive allosteric modulator at GABAA receptors, penetrates the blood-brain barrier, and possesses anticonvulsant activity in the central nervous system (CNS) [27]. Lin et al. further reported that in Hispidulin-treated glioblastoma (GBM) cells, the activation of AMP-activated protein kinase (AMPK) suppressed protein synthesis, lipogenesis, and cell cycle progression. Their results suggested that Hispidulin might be useful as a chemopreventive or therapeutic agent for GBM. Subsequent observations indicated that Hispidulin is a potential modulator of CNS activity, prompting our own investigation of its antineoplastic activity against GBM [28].

In this study, we identified that Hispidulin treatment markedly upregulated *NAG-1* protein expression and downregulated COX-2 protein expression significantly, in AGS gastric cancer cells. After various durations of exposure of cells to Hispidulin, the expression of *EGR-1* and that of *NAG-1* was upregulated in a time-dependent manner. Hispidulin treatment also increased ERK1/2 activity, and an ERK1/2 inhibitor markedly downregulated the expression of *NAG-1* and the growth inhibitory effects of Hispidulin in AGS cells. These results suggested that the apoptotic effects of Hispidulin in human gastric cancer cells might be directly associated with the upregulation of *NAG-1* expression through ERK1/2 activation. Our findings indicate that Hispidulin exerts therapeutic effects on human gastric cancer cells through the activation of *NAG-1* through the ERK1/2 signaling pathway.

## 2. Materials and Methods

**2.1. Preparation of Fractions.** The wild plant of *S. involucreata* used in this study was a gift from Biopure Biotechnology (Changhua, Taiwan). Twenty grams of dried and powdered aerial parts, including flower, of *S. involucreata* was extracted with 100 mL of methanol three times under reflux for 2 h, respectively. The methanol extracts (SI-1) were combined, and the solvent was evaporated in vacuum to give a deep brown syrup. The syrup was resuspended in water and then partitioned successively with pentane, ethyl acetate (SI-2), and n-butanol (SI-3) to leave a water layer (SI-4). The solvents were evaporated, respectively, and the residues were used throughout this study.

**2.1.1. Reverse-Phase High-Performance Liquid Chromatography (HPLC) Analysis of Flavonoids in *S. involucreata*.** The determination of flavonoids from *S. involucreata* was carried out by HPLC with a photodiary detector. The HPLC system consisted of a Shimadzu LC-20AT solvent delivery system, equipped with a SPD-M20A photodiode array detector, set at 270 nm. Samples were injected with SiL-20A autosample to separate on the TSK-Gel ODS-100S column. The column was maintained at an ambient temperature of 25°C. The flow rate of the system was 1.0 mL/min. The mobile phase consisted of solvent A (0.3% formic acid) and solvent B (acetonitrile). The elution profile for A was 0–10 min, with a linear gradient change of 0–5%; 10–40 min, with a linear gradient change to 55%; and maintained for another 10 min with a postrun time

to equilibrate the column and for the baseline to return to the normal and initial working conditions.

**2.2. Chemicals and Reagents.** Rutin was dissolved in DMSO to a concentration of 50 mM and stored in  $-20^{\circ}\text{C}$  as a master stock solution. Dimethyl sulfoxide (DMSO), 3-(4,5-dimethylthiazol-2-yl)-2,5-diphenyl tetrazolium bromide (MTT), 2',7'-dichlorofluorescein diacetate ( $\text{H}_2\text{DCF-DA}$ ), Hoechst 33342, thiobarbituric acid (TBA), hydrogen peroxide ( $\text{H}_2\text{O}_2$ ), trichloroacetic acid (TCA), malondialdehyde (MDA), propidium Iodide (PI), and actin antibody were purchased from Sigma-Aldrich (St. Louis, MO, USA). NuPAGE Bis-Tris Electrophoresis System (precast polyacrylamide minigel) was purchased from Invitrogen (Carlsbad, CA, USA). COX-2 antibody was purchased from Thermo scientific (Waltham, MA, USA). PARP antibodies and horseradish peroxidase-conjugated anti-mouse or anti-rabbit IgG secondary antibodies were purchased from Cell signaling (MA, USA). Polyvinylidene fluoride (PVDF) membranes, BSA protein assay kit, and Western blot chemiluminescence reagent were purchased from Amersham Biosciences (Arlington Heights, IL). Superoxide dismutase activity assay kit was purchased from biovision (Mountain View, CA). Glutathione peroxidase assay kit was purchased from Cayman Chemical (MI, USA). DNA Fragmentation Assay Kit was purchased from Clontech Laboratories (Mountain View, CA). Nonradioactive Cytotoxicity Assay was purchased from promega (Madison, WI, USA).

**2.3. Cell Lines and Cell Culture.** AGS human gastric adenocarcinoma cell line (ATCC, CRL-1739) were obtained from American Type Culture Collection (Manassas, VA) and propagated in culture dishes at the desired densities in RPMI 1640 medium supplemented with 10% fetal bovine serum and 1% penicillin/streptomycin. The cells were incubated at  $37^{\circ}\text{C}$  in a humidified atmosphere containing 5%  $\text{CO}_2$ .

**2.4. Growth Inhibition Assay.** The viability of the cells after treatment with various chemicals was evaluated using the MTT assay preformed in triplicate. Briefly, the cancer cells ( $3 \times 10^3$ ) were incubated in 96-well plates containing  $200 \mu\text{L}$  of the culture medium. Cells were permitted to adhere for 12–18 h then washed with phosphate-buffered saline (PBS). Solutions were always prepared fresh by dissolving 0.2% DMSO or drugs in culture medium and then were added to AGS cells. For inhibitor treatment experiments, cells were treated with  $50 \mu\text{M}$  Hispidulin and preincubated for 1 h with 25 and  $50 \mu\text{M}$  ERK1/2 inhibitor PD98059. After 48 h of exposure, the drug-containing medium was removed, washed with PBS, and replaced by fresh medium. The cells in each well were then incubated in culture medium with  $500 \mu\text{g}/\text{mL}$  MTT for 4 h. After the medium was removed,  $200 \mu\text{L}$  of DMSO and  $25 \mu\text{L}$  of glycine buffer (0.1 M glycine and 0.1 M NaCl, pH 10.5) were added to each well. Absorbance at 570 nm of the maximum was detected by a PowerWave X Microplate ELISA Reader (Bio-Tek Instruments, Winooski, VT). The absorbance for DMSO-treated cells was considered as 100%. The results were determined by three independent experiments.

**2.5. IC50 Determination.** MTT assay was according to the paper [29]. Briefly, the pale yellow redox indicator 3-(4,5-dimethylthiazol-2-yl)-2,5-diphenyl tetrazolium bromide (MTT) is reduced to a dark blue end product, MTT-Formazan, by the mitochondrial dehydrogenases of living cells. MTT reduction can be measured spectrophotometrically at a wavelength of 570 nm. According to the dosage dependent curve, the MTT reduction half was indicated IC50. In our study, Hispidulin is resolved on DMSO agent with final concentration 0.2%. Therefore, we used 0.2% DMSO as a control agent. The absorbance for DMSO treated cells without adding any drugs was considered as 100%.

**2.6. Cell Cycle Analysis.** The cell cycle was determined by flow cytometry with DNA staining to reveal the total amount of DNA. Approximately  $5 \times 10^5$  of cells were incubated in various concentrations of Hispidulin for the indicated time. Cells were harvested by treating the cells with trypsin/EDTA. The cells were collected, washed with PBS, fixed with cold 70% ethanol overnight, and then stained with a solution containing  $20 \mu\text{g}/\text{mL}$  PI and 0.1% Triton X-100 for 1 h in the dark. The cells will then pass through FACScan flow cytometer (equipped with a 488-nm argon laser) to measure the DNA content. The data was obtained and analyzed with Cell Quest 3.0.1 (Becton Dickinson, Franklin Lakes, NJ) and Mod FitLT V2.0 software.

**2.7. Western Blot Analysis.** Approximately  $5 \times 10^6$  cells were cultured in  $100 \text{ mm}^2$  dishes and then incubated in various concentration of Hispidulin for 48 h. The cells were lysed on ice with 150 mL of lysis buffer (50 mmol/L Tris-HCl, pH 7.5, 0.5 mol/L NaCl, 5 mmol/L  $\text{MgCl}_2$ , 0.5% nonidet P-40, 1 mmol/L phenylmethylsulfonyl fluoride, 1 mg/mL pepstatin, and 50 mg/mL leupeptin) and centrifuged at  $13000 \times g$  at  $4^{\circ}\text{C}$  for 15 min. The protein concentrations in the supernatants were quantified using a BSA Protein Assay Kit. Electrophoresis was performed on a NuPAGE Bis-Tris Electrophoresis System using 50 mg of reduced protein extract per lane. Resolved proteins were then transferred to polyvinylidene fluoride (PVDF) membranes. Filters were blocked with 5% nonfat milk overnight and probed with appropriate dilution of primary antibodies for 2 h at room temperature. Membranes were washed with three times with 0.1% Tween 100 and incubated with HRP-conjugated secondary antibody for 1 h at room temperature. All proteins were detected using Western Lightning chemiluminescence reagent plus and quantified using a densitometer.

**2.8. Detection of Apoptosis.** The viability of the cells after treatment with various chemicals was evaluated using an MTT assay preformed in triplicate. Briefly, the cancer cells ( $5 \times 10^3$ ) were incubated in 96-well plates containing  $200 \mu\text{L}$  of serum-containing medium. Cells were permitted to adhere for 12 to 18 h and then were washed with phosphate-buffered saline (PBS). Solutions were always prepared fresh by dissolving 0.2% DMSO or drugs in culture medium and added to AGS cells. For inhibitor treatment experiments, cells were treated with  $50 \mu\text{M}$  Hispidulin and preincubated for 1 h



with ERK1/2 inhibitor PD98059. After 24 h of exposure, the drug-containing medium was removed, washed with PBS, and replaced by fresh medium. The apoptosis was analyzed according to the method described by van Engeland et al. [30] to detect the integrity of cellular membrane and the externalization of phosphatidylserine (Cytometry 1998; 31:1–9). In brief, approximately  $1 \times 10^6$  cells were grown in 10 mm diameter plates. The cells were incubated in various concentrations of K8 for the indicated time and then labeled with FITC Annexin V and PI prior to harvesting. After labeling, the cells were washed with binding buffer and harvested by scraping. Cells were resuspended in binding buffer at a concentration of  $2 \times 10^5$  cells/mL before analysis by flow cytometry (FACScan). The data was analyzed on WinMDI V2.8 software. The percentage of cells undergoing apoptosis was determined by three independent experiments.

**2.9. Caspase Activity Assay.** Activity of caspase-3 was detected by using a fluorometric assay kit (Promega) according to the manufacturer's protocol. In brief,  $2 \times 10^6$  control or treated cells were lysed in 50  $\mu$ L of cold lysis buffer and incubated in ice for 10 min. Fifty microliters of cell lysates was added to 50  $\mu$ L of reaction buffer and 5  $\mu$ L of fluorogenic report substrates specific for caspase-3 in a 96-well microplate. After incubation at 37°C for 1 h, the fluorescence from the cleaved C-terminal side of the aspartate residue of DEVD-7-amino-4-trifluoromethyl coumarin was detected by a fluorescence microplate reader (Fluoroskan Ascent; Thermo Fisher Scientific, Waltham, MA), with excitation at 400 nm and emission at 505 nm.

**2.10. Statistical Analysis.** The data was shown as mean with standard deviation. The statistical difference was analyzed using the Student's *t*-test for normal, distributed values and by nonparametric Mann-Whitney *U* test for values of nonnormal distribution. Values of  $P < 0.05$  were considered significant.

### 3. Results

**3.1. Hispidulin Inhibits Human Gastric Cancer Cell Growth.** To test the inhibitory effect of Hispidulin (40,5,7-trihydroxy-6-methoxyflavone) on cancer cell, we treated human gastric cancer AGS cells with Hispidulin. Twenty-four, 48, and 72 hours after treatment followed by MTT cell viability assay, we observed that Hispidulin displayed significantly higher cytotoxicity to AGS cells than other drugs such as rutin and Aspirin (Figure 1). The IC<sub>50</sub> of Hispidulin to AGS cell was 50  $\mu$ M at 48 h after treatment and 20  $\mu$ M at 72 h after treatment (Figure 1(a)). On the other hand, the IC<sub>50</sub> of rutin, a main component of *Saussurea involucreata* that can attenuate the senescence [21], was over 500  $\mu$ M (Figure 1(b)). Since cyclooxygenase-2 (COX-2) was often overexpressed in gastric adenocarcinomas, we also treated AGS cells with COX-2 inhibitor (celecoxib or NS-398). The results indicated that the IC<sub>50</sub> of celecoxib and NS-398 were around 40  $\mu$ M and 50  $\mu$ M 48 h after treatment and 30  $\mu$ M and 40  $\mu$ M 72 h after treatment, respectively, (Figures 1(c)–1(d)). However, treated

AGS cells with COX-1 inhibitor, Aspirin, had less inhibitory effect on cell viability (IC<sub>50</sub> > 1 mM) (Figure 1(e)). Taken together, Hispidulin can be more effective in gastric cancer survival inhibition than well-known COX-2 inhibitors.

**3.2. Hispidulin Induces AGS Cells Apoptosis and G1/S Phase Cell Cycle Arrest.** We then evaluated the association between Hispidulin-induced inhibition of cell growth and induction of apoptosis. After Hispidulin treatment, the percentage of cell apoptosis was significantly elevated in dose and time-dependent manners (Figure 2(a)). In addition, activation of caspase-3 was also significantly induced with dose-dependent phenomena (Figure 2(b)). Furthermore, caspase-3 was activated significantly 24 to 48 h after Hispidulin treatment (Figure 2(c)), and the caspase-3 mediated apoptosis was attenuated by pan caspase-3 inhibitor FMK (Figures 2(b)–2(c)). These results indicated that the apoptosis effect by Hispidulin on AGS cell line was a caspase-dependent manner. The western blot analysis also more supported that Hispidulin induced apoptosis included activation of caspase-9, cleavage of caspase-3, and poly (ADP-ribose) polymerase (PARP) with in time- and dose-dependent manners (Figures 2(d)–2(e)).

**3.3. Hispidulin Induces AGS Cell Cycle Arrest during the G1/S Phase.** To elucidate the mechanisms underlying the activities of Hispidulin, we evaluated its effects on cell cycle progression. Our results from flow cytometric analysis showed that Hispidulin treatment induced the accumulation of cells in the G1/S phase in a time-dependent manner (Figure 3(a)). This result suggested that Hispidulin might induce G1/S phase arrest, similar to fluorouracil (5-FU). Hispidulin also upregulated the expression of the G1/S regulatory proteins, including p53, p16, and p21, in time- and dose-dependent manners (Figure 3(b)). Hispidulin treatment downregulated the expression of the cell cyclin-associated proteins, including cyclin D1 and cyclin E, in AGS cells (Figure 3(b)).

**3.4. Involvement of NAG-1 Activation and COX-2 Inhibition in Hispidulin-Induced Inhibition of AGS Cell Growth.** The IC<sub>50</sub> for Hispidulin was 50  $\mu$ M in AGS cells (Figure 1(a)); therefore, we used the same concentration in this study's experiments. To evaluate the involvement of EGR-1 in the upregulation of NAG-1 expression induced by Hispidulin treatment in AGS cells, we used western blotting to analyze EGR-1 and NAG-1 protein expression. After various durations of exposure of cells to Hispidulin, the expression of EGR-1, as well as NAG-1, was upregulated in a time-dependent manner. EGR-1 was upregulated significantly after 6 h treatment and this effect remained until 24 h treatment. NAG-1 expression peaked after 48 h Hispidulin treatment. Hispidulin treatment markedly downregulated COX-2 expression and NF-kappa B subunit p65 expression in AGS cells (Figure 4).

**3.5. The Involvement of ERK1/2 Signaling in the Hispidulin-Induced Upregulation of EGR-1 and NAG-1 Expression.** To investigate the possible role of ERK1/2 in the regulation of EGR-1 and NAG-1, we treated AGS cells with Hispidulin in

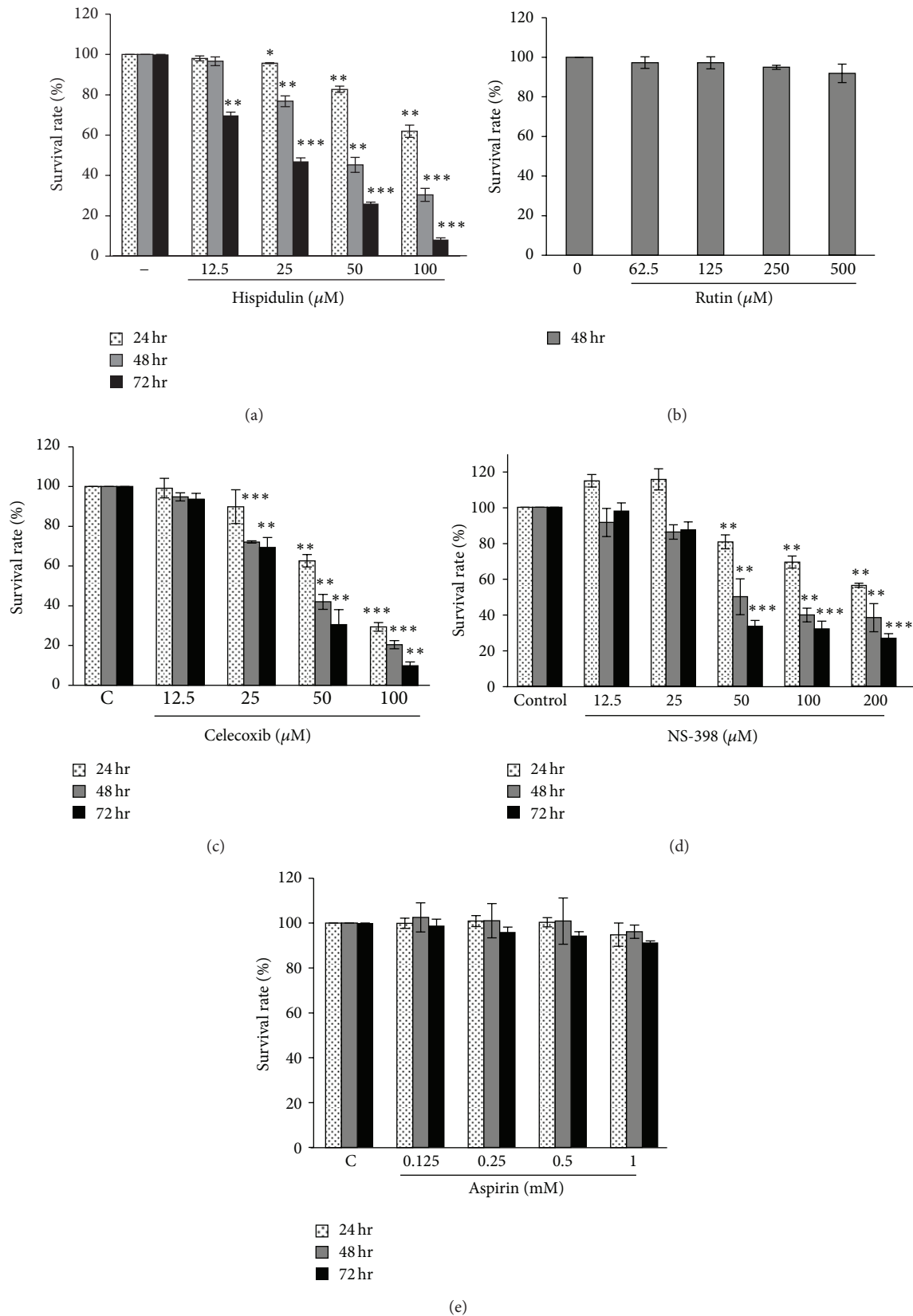


FIGURE 1: Hispidulin can efficiently inhibit gastric cancer cell growth. (a) Cell viability after Hispidulin treatment. (b) Cell viability after rutin treatment. (c) Cell viability after COX-2 inhibitor, celecoxib, treatment. (d) Cell viability after COX-2 inhibitor, NS-398, treatment. (e) Cell viability after COX-1 inhibitor, Aspirin, treatment. Each column represents the mean  $\pm$  SD (\*  $P < 0.05$ ; \*\*  $P < 0.01$ ; \*\*\*  $P < 0.001$ ).

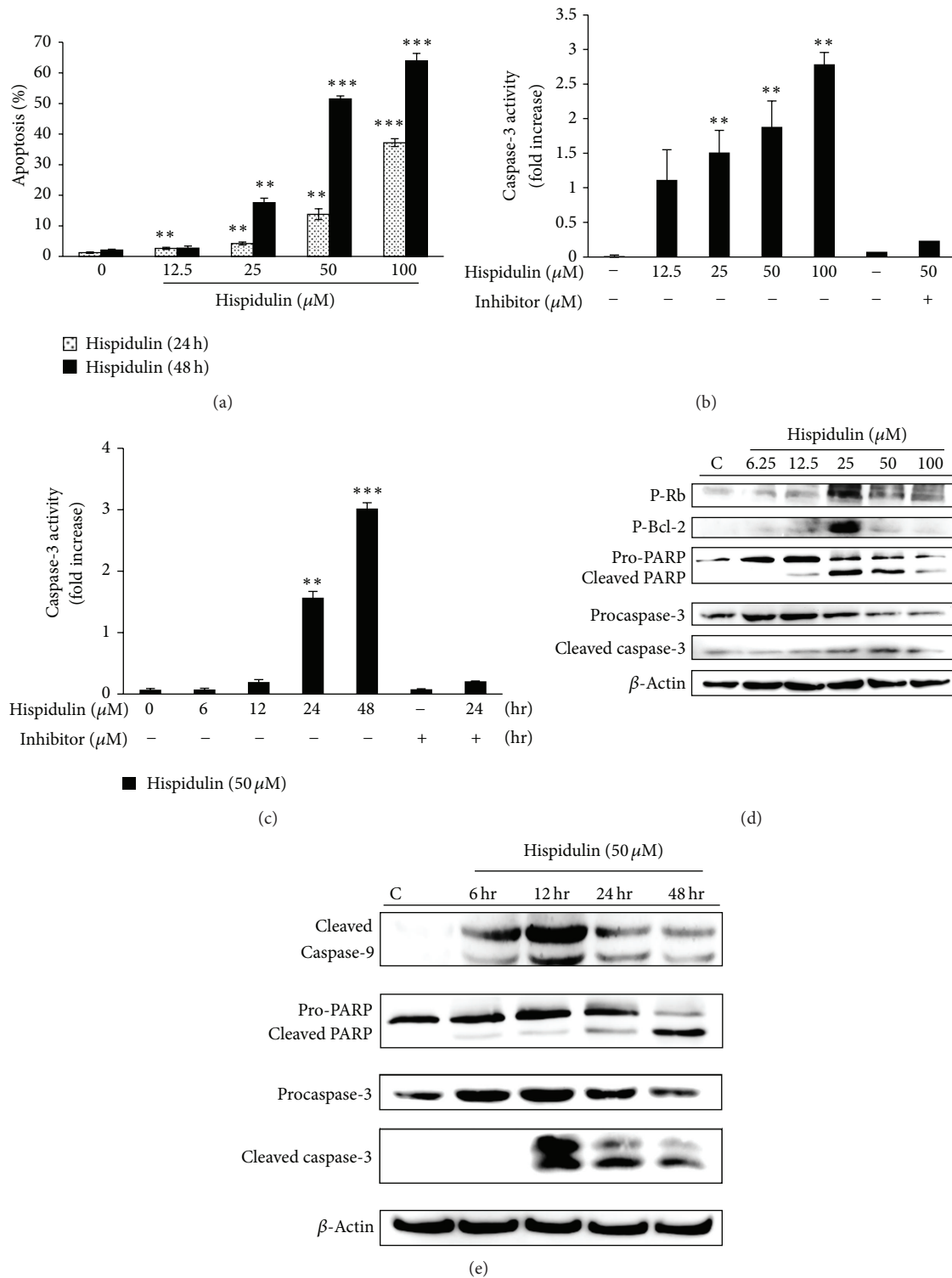


FIGURE 2: Hispidulin can induce cancer apoptosis by caspase-3 activation. (a) Cell apoptosis assay after treatment by flow cytometry apoptosis analysis. (b) Caspase-3 activity assay after treatment in various dosage. (c) Caspase-3 activity assay 6, 12, 24, and 48 h after 50  $\mu\text{M}$  Hispidulin treatment. (d) The Western blot analysis for apoptosis related protein analysis after Hispidulin treatment. Expression of  $\beta$ -actin was used as an internal control. (e) The Western blot analysis for apoptosis related protein analysis 6, 12, 24, and 48 h after treatment. Expression of  $\beta$ -actin was used as an internal control. Each column represents the mean  $\pm$  SD (\* $P$  < 0.05; \*\* $P$  < 0.01; \*\*\* $P$  < 0.001).

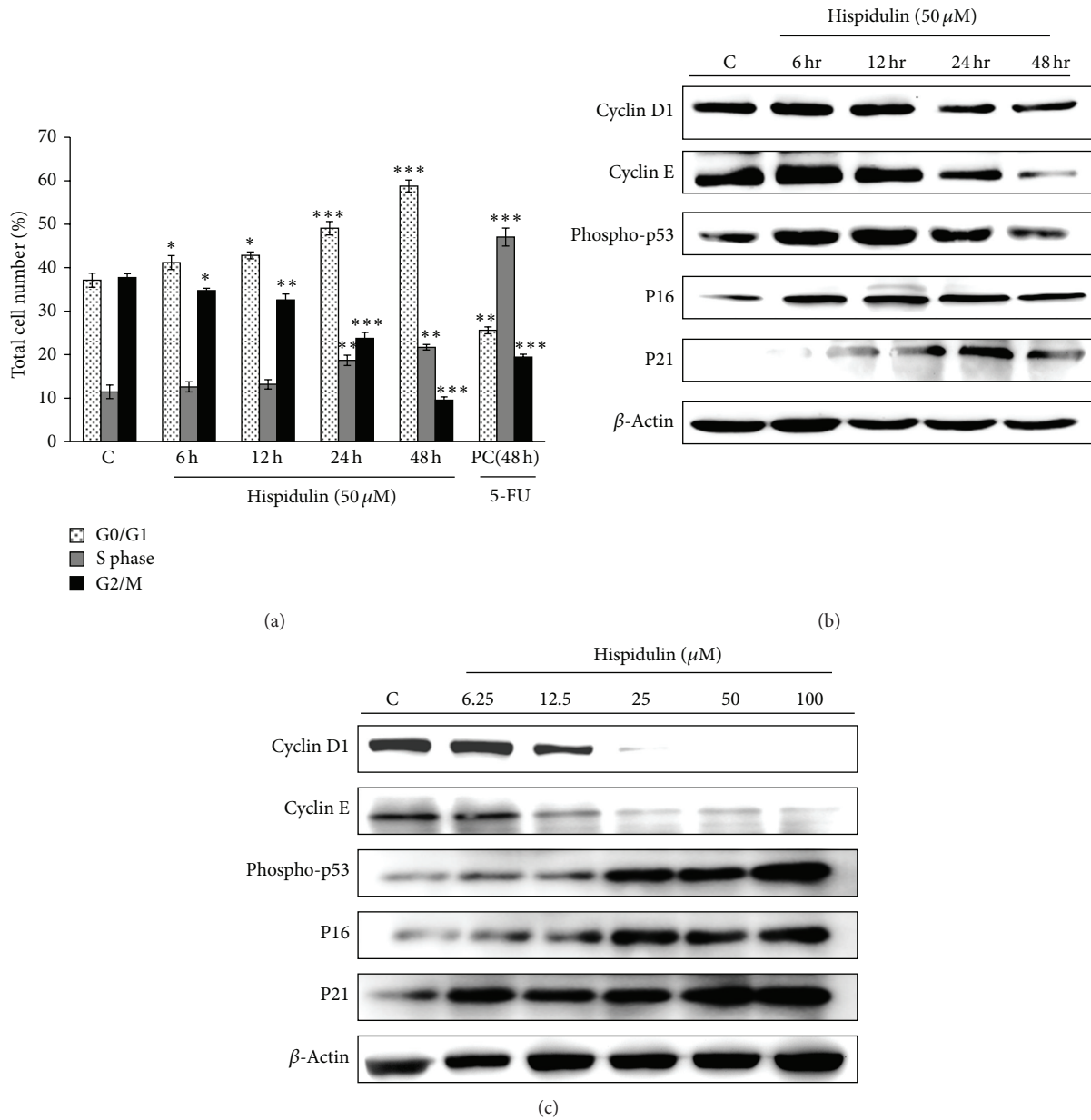


FIGURE 3: Effect of Hispidulin-induced G1/S phase arrest and changes expression of G1/S regulatory proteins in AGS cells. (a) The cell cycle analysis 6–48 h after Hispidulin treatment. (b) The Western blot analysis for p16, p21, cyclin D1, and cyclin E expression 6–48 h after treatment. Expression of  $\beta$ -actin was used as an internal control. (c) The western blot analysis for p16, p21, cyclin D1, and cyclin E expression in various dosage treatments. Expression of  $\beta$ -actin was used as an internal control. Each column represents the mean  $\pm$  SD (\* $P$  < 0.05; \*\* $P$  < 0.01; \*\*\* $P$  < 0.001).

the presence and absence of the MEK1/2 inhibitor PD98059 (25  $\mu$ M and 50  $\mu$ M), the p38 inhibitor SB203580 (10  $\mu$ M and 20  $\mu$ M), or the JNK1/2 inhibitor SP600125 (10  $\mu$ M and 20  $\mu$ M). PD98059 reduced the growth inhibitory effects of Hispidulin in a dose-dependent manner (Figure 5(a)). We then investigated the effects of Hispidulin on MAPK activation to establish which MAPK pathways are involved in its growth inhibitory effects. Following the exposure of AGS cells to Hispidulin, we observed the upregulation of phosphor-ERK protein expression (Figure 5(b)). Using

western blot analysis, we then identified that the inhibition of ERK1/2 expression by PD98059 induced the downregulation of EGR-1, NAG-1, and COX-2 protein expression, and reduced growth inhibition, in a dose-dependent manner in Hispidulin-treated AGS cells (Figures 5(c) and 5(d)). In contrast, inhibition of JNK1/2 exerted minimal effects on NAG-1 expression, whereas inhibition of p38 did not affect the expression of the 2 genes. These results suggested that the activation of the ERK1/2 signaling pathway is involved in the upregulation of EGR-1 and NAG-1 expression by

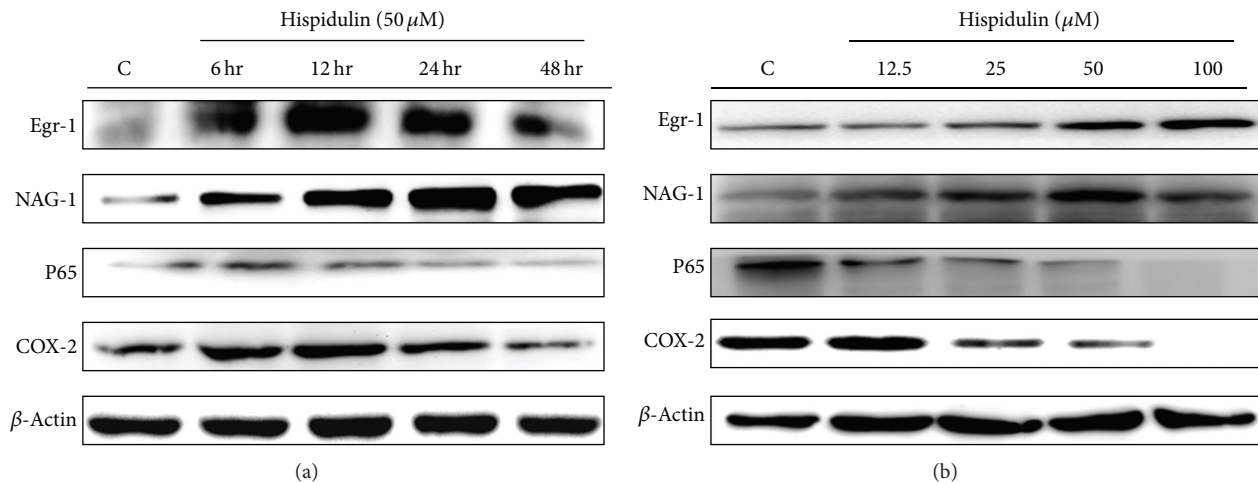


FIGURE 4: Effect of Hispidulin on NAG-1 signaling associated protein expression in AGS cells. (a) NAG-1 related signaling analysis 6–48 h after treatment. The expression of  $\beta$ -actin was used as an internal control. (b) NAG-1 related signaling analysis 48 h after various dosage treatments. The expression of  $\beta$ -actin was used as an internal control.

Hispidulin. Taken together, Hispidulin can efficiently inhibit cancer cell survival through apoptosis induction via ERK1/2, NAG-1 mediated pathway. Thus, it can be applied to clinically combined treatment for gastric cancer elimination (Figure 6).

#### 4. Discussion

NSAIDs are effective chemopreventive agents for various cancers via the inhibition effect on prostaglandin synthesis. Previous studies identified the chemopreventive and antitumorogenic activities of NSAIDs against colorectal and other human cancers; however, the molecular mechanisms responsible for these properties have yet to be fully elucidated [31–33]. It has been reported that *NAG-1* is a target gene for NSAIDs and a unique member of the transforming growth factor superfamily. Increases in *NAG-1* expression result in the induction of apoptosis in several cancer cell lines [14, 16]. Also, *NAG-1* expression is induced not only by NSAIDs but also by several antitumorogenic compounds. These include dietary compounds, peroxisome proliferatoractivated receptor- $\gamma$  ligands, and phytochemicals [34, 35] as well as resveratrol, genistein, diallyl disulfide, 5F203, and retinoid 6-[3-(1-adamantyl)-4-hydroxyphenyl]-2-naphthalene carboxylic acid [17, 36, 37]. In our previous study, we also found that a novel lignin, isochaihuactone, increased *NAG-1* mRNA and protein expression and inhibited cell proliferation on human lung cancer A549 cells. In this study, we reported that the flavonoid Hispidulin upregulates the expression of the proapoptotic and antitumorogenic protein *NAG-1*. Our results indicated that *NAG-1* is an important target gene for Hispidulin. Our study results could increase understanding of the mechanisms by which Hispidulin can affect tumor development. During our analyses, we observed the Hispidulin-induced upregulation of *NAG-1* expression in the human AGS gastric cancer cell line had relatively reduced COX-2 activity repression. Our results demonstrated that Hispidulin-treated cells had *NAG-1* elevated expression and

reduced COX-2 expression. However, the regulatory relationship between *NAG-1* and COX-2 still remained to be investigated although many anticancer drugs and compounds had effects on *NAG-1* and COX-2 at the same treatment [20, 28]. Since COX-2 overexpression had relative malignance in clinical gastric cancer patients, this finding provide a potency that Hispidulin can be served as an adjuvant therapy.

Expression of iNOS and COX-2 is largely regulated by transcriptional activation. Among these transcription factors, NF- $\kappa$ B, which is a primary transcription factor and regulates various genes, is critical in the inflammation [38]. NF- $\kappa$ B is a redox-sensitive transcription factor that regulates a multitude of inflammatory genes, including cytokines, chemokines, adhesion molecules, and acute phase proteins. Under basal conditions, NF- $\kappa$ B is inactive and prevented from DNA binding and nuclear translocation by tight association in the cytoplasm with inhibitory proteins. Cell activation by a variety of extracellular signals, such as oxidative stress, induces a cascade of events that lead to activating NF- $\kappa$ B then translocating it to the nucleus where it binds to DNA elements in the promoters of numerous proinflammatory gene families [21, 39]. In our study, after treatment with hispidulin, the expression of nuclear factor  $\kappa$ B (NF- $\kappa$ B)-p65 in cytoplasm extract fractions decreased, as compared to that of the control (Figure 4). Taken together, the results suggest that hispidulin may exert anti-inflammatory effects *in vitro* in AGS cells through inhibition of NF- $\kappa$ B signal pathway activation. Induction of EGR-1 expression by anti-tumorogenic compounds is known to involve members of the family of mitogen-activated protein kinases (MAPKs) or phosphatidylinositol-3-kinase (PI3K) dependent pathways. For example, induction of EGR-1 expression by the peroxisome proliferator- $\gamma$  activated receptor- $\gamma$  (PPAR $\gamma$ ) ligand troglitazone occurs by the ERK phosphorylation pathway rather than by the PPAR $\gamma$  pathway [15, 16].

To determine which MAPK family is involved in the major signaling pathway for Hispidulin-mediated *NAG-1*



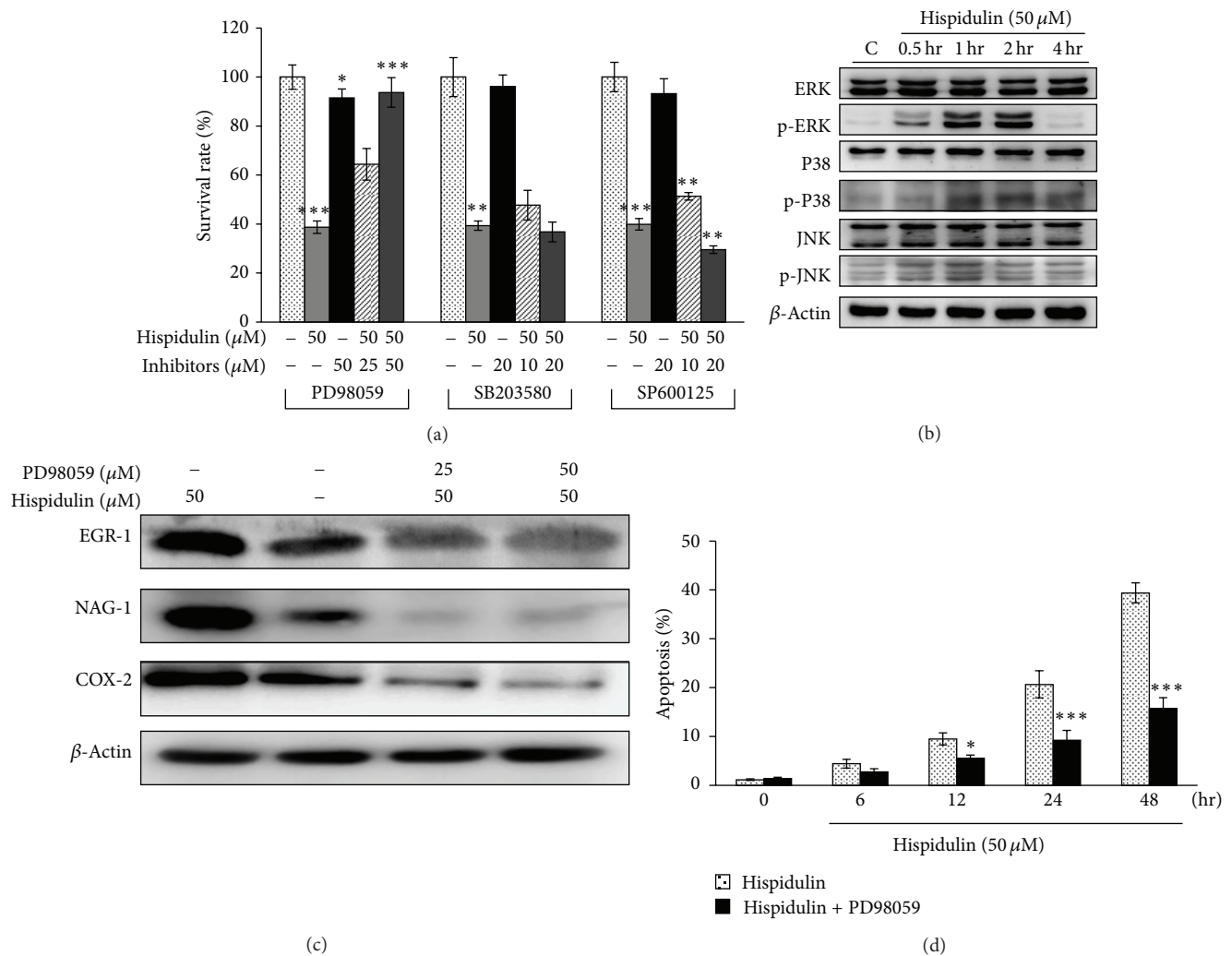


FIGURE 5: Inhibition of NAG-1 expression and growth inhibition by ERK1/2 inhibitor. (a) AGS cells were treated with 30  $\mu\text{M}$  Hispidulin in the presence or absence of the mitogen-activated protein kinase kinase 1/2 inhibitor PD98059, p38 inhibitor SB203580, and JNK1/2 inhibitor SP600125. For 48 h incubation, growth inhibition effect was determined by MTT assay. (b) AGS cells were treated with 30  $\mu\text{M}$  Hispidulin for the indicated times. Total ERK1/2, phosphor-ERK1/2 (pERK1/2), total p38, phosphor-p38 (pp38), total JNK, and phosphor-JNK (pJNK) were detected by Western blot. (c) Attenuation of Hispidulin-induced NAG-1 upregulation in AGS cells by ERK inhibitor PD98059. AGS cells where treatment with 25–50  $\mu\text{M}$  of PD98059 and NAG-1 expression was evaluated by Western blot analysis. (d) Apoptosis induced by Hispidulin was attenuated by PD98059 ERK inhibitor treatment followed by flow cytometry analysis. Each column represents the mean  $\pm$  SD (\* $P < 0.05$ ; \*\* $P < 0.01$ ; \*\*\* $P < 0.001$ ). Expression of  $\beta$ -actin was used as an internal control.

upregulation and growth inhibition, we applied MAPK inhibitors to Hispidulin-treated AGS cells. The ERK inhibitor PD98059 reduced the growth inhibitory effects of Hispidulin significantly (Figure 5(a)); however, the p38 inhibitor SB203580 and the JNK inhibitor SP600125 did not limit its growth inhibitory effects in AGS cells (data not shown). The ERK1/2 inhibitor PD98059 was the sole compound to reduce Hispidulin-induced upregulation of EGR-1 and NAG-1 protein expression (Figure 5(c)). These data support the concept that Hispidulin-induced ERK1/2 activity is critically involved in the regulation of EGR-1 and NAG-1 expression.

In an attempt to identify the signaling pathway through which PI3K/AKT/GSK3 $\beta$  is involved in receptor signal transduction through tyrosine kinase receptors for hispidulin,

the effect of LY294002, a PI3K inhibitor, was examined. We found that LY294002 did not reverse tumor growth inhibition caused by hispidulin (data not shown). Compared with the effects of other phytochemical agents, this result suggests that the ability of our drug to cause tumor apoptosis might not go through this pathway. Results from analyses of COX-2 protein expression in AGS cells following their treatment with Hispidulin showed that Hispidulin induced morphological changes in the AGS cells (data not shown), inhibited AGS cell growth (Figure 1(a)), and arrested the cell cycle at the G1/S phase (Figure 3(a)). The tumor suppressor protein p53 plays a role in the molecular response to DNA damage. Acting as a DNA-binding transcription factor, it regulates specific target genes to arrest the cell cycle and initiate apoptosis. Following

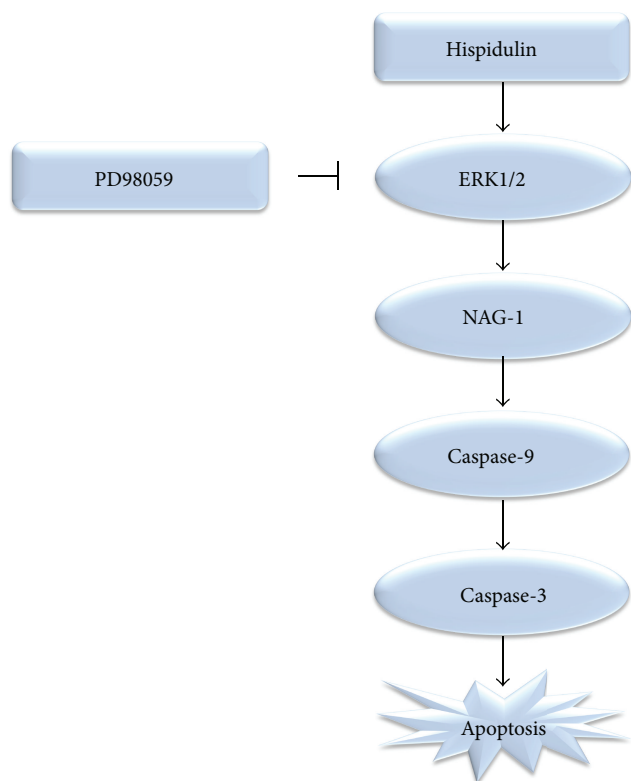


FIGURE 6: Hypothetic mechanism of signaling for gastric cancer inhibition by Hispidulin. Hispidulin can efficiently activate ERK1/2 signaling followed by NAG-1 constitutive expression and trigger cell cycle arrest as well as apoptosis in cancer cell.

DNA damage, the cyclin-dependent kinase inhibitor p21 is upregulated in a p53-dependent or p53-independent manner. The p21 might assist with the maintenance of G1 cell cycle arrest by inactivating the cyclin D1/cyclin E complex, leading to the phosphorylation of the Rb protein. In this study, Hispidulin treatment upregulated phospho-p53, p16, and p21 expression in AGS cells (Figure 3(b)). Our findings indicated that Hispidulin mediates AGS cell arrest at the G1/S phase (Figure 3(a)), with cell arrest accompanied by the downregulation of cyclin D1 and cyclin E expression. These results suggested that Hispidulin treatment causes inappropriate accumulation of G1/S regulators leading to apoptosis.

Hispidulin induces apoptosis in A549 cells following mitotic arrest. The mechanism by which microtubule-damaging agents induce apoptosis is not well understood. The activation of aspartate-specific cysteine protease (caspase) represents a crucial step in the induction of drug-induced apoptosis, with the cleavage of PARP by caspase-3 considered one of the hallmarks of apoptosis. In this study, the pan caspase-3 inhibitor FMK reduced the apoptosis-promoting effects of Hispidulin (Figures 2(b) and 2(c)). These results suggested that a caspase-dependent pathway mediates Hispidulin-induced apoptosis (Figures 2(d)-2(e)) and cell death. In our experiments, Hispidulin induced caspase-9 activation, Bcl-2 phosphorylation, and cleavage of caspase-3 and PARP in a time-dependent manner (Figures 2(d)-2(e)).

In summary, Hispidulin is a novel flavonoid compound that has modulatory effects on the expression of cyclin D1/cyclin E G1/S regulatory proteins and initiates the apoptotic cascade [19, 20]. Our study findings show that NAG-1 displays anti-tumorigenic and proapoptotic activities *in vitro* and indicate that Hispidulin, regulates NAG-1 expression. Although further detailed analyses are required to fully elucidate the mechanisms underlying the antitumorigenic effects of Hispidulin these results should encourage further investigation of Hispidulin as a potential novel clinical anticancer drug.

## Abbreviations

|         |  |
|---------|--|
| NAG-1:  | NSAID-activated gene-1   |
| K8:     | Isochaulactone   |
| RT-PCR: | Reverse transcription-polymerase chain reaction                |
| DMSO:   | Dimethyl sulfoxide   |
| PBS:    | Phosphate-buffered saline                                      |
| PCR:    | Polymerase chain reaction                                      |
| MTT:    | 3-(4,5-dimethyl thiazol-2-yl)-2,5-diphenyl tetrazolium bromide |
| PVDF:   | Polyvinylidene fluoride  |
| MBD:    | Methyl-CpG binding domain                                      |
| NSAIDs: | Anti-inflammatory drugs  |
| CI:     | Combination index  |
| FBS:    | Fetal bovine serum   |
| IHC:    | Immunohistochemical.   |

## Conflict of Interests

All of the authors indicated no potential conflict of interests relevant to this paper.

## Authors' Contribution

Due-Chuan Chan and Yi-Lin Sophia Chen contributed equally to this work.

## Acknowledgments

This work was supported by a Grant from National Science Council of the Republic of China (101-2320-B-197-001-MY2) and Tri-Service General Hospital, Taipei, Taiwan TSGH-C101-020.

## References

- [1] J. R. Kelley and J. M. Duggan, "Gastric cancer epidemiology and risk factors," *Journal of Clinical Epidemiology*, vol. 56, no. 1, pp. 1-9, 2003.
- [2] J.-Y. Shin, J.-O. Kim, S. K. Lee, H.-S. Chae, and J.-H. Kang, "LY294002 may overcome 5-FU resistance via down-regulation of activated p-AKT in Epstein-Barr virus-positive gastric cancer cells," *BMC Cancer*, vol. 10, article 425, 2010.
- [3] M. R. Baeza, T. O. Giannini, S. R. Rivera et al., "Adjuvant radiochemotherapy in the treatment of completely resected, locally advanced gastric cancer," *International Journal of Radiation Oncology, Biology, Physics*, vol. 50, no. 3, pp. 645-650, 2001.

- [4] S. Cascinu, M. Scartozzi, R. Labianca et al., "High curative resection rate with weekly cisplatin, 5-fluorouracil, epidoxorubicin, 6S-leucovorin, glutathione, and filgrastim in patients with locally advanced, unresectable gastric cancer: a report from the Italian Group for the Study of Digestive Tract Cancer (GISCAD)," *British Journal of Cancer*, vol. 90, no. 8, pp. 1521–1525, 2004.
- [5] D. B. Longley, D. P. Harkin, and P. G. Johnston, "5-fluorouracil: mechanisms of action and clinical strategies," *Nature Reviews Cancer*, vol. 3, no. 5, pp. 330–338, 2003.
- [6] C. J. Buskens, B. P. van Rees, A. Sivula et al., "Prognostic significance of elevated cyclooxygenase 2 expression in patients with adenocarcinoma of the esophagus," *Gastroenterology*, vol. 122, no. 7, pp. 1800–1807, 2002.
- [7] N. Kim, C. H. Kim, D.-W. Ahn et al., "Anti-gastric cancer effects of celecoxib, a selective COX-2 inhibitor, through inhibition of Akt signaling," *Journal of Gastroenterology and Hepatology*, vol. 24, no. 3, pp. 480–487, 2009.
- [8] Y. Kishimoto, K. Yashima, T. Morisawa, G. Shiota, H. Kawasaki, and J. Hasegawa, "Effects of cyclooxygenase-2 inhibitor NS-398 on APC and c-myc expression in rat colon carcinogenesis induced by azoxymethane," *Journal of Gastroenterology*, vol. 37, no. 3, pp. 186–193, 2002.
- [9] H. Y. Lim, H. J. Joo, J. H. Choi et al., "Increased expression of cyclooxygenase-2 protein in human gastric carcinoma," *Clinical Cancer Research*, vol. 6, no. 2, pp. 519–525, 2000.
- [10] J. Houghton, J. G. Fox, and T. C. Wang, "Gastric cancer: laboratory bench to clinic," *Journal of Gastroenterology and Hepatology*, vol. 17, no. 4, pp. 495–502, 2002.
- [11] X. M. Fan, B. C. Y. Wong, M. C. M. Lin et al., "Interleukin-1 $\beta$  induces cyclo-oxygenase-2 expression in gastric cancer cells by the p38 and p44/42 mitogen-activated protein kinase signaling pathways," *Journal of Gastroenterology and Hepatology*, vol. 16, no. 10, pp. 1098–1104, 2001.
- [12] S. J. Baek, L. C. Wilson, and T. E. Eling, "Resveratrol enhances the expression of non-steroidal anti-inflammatory drug-activated gene (NAG-1) by increasing the expression of p53," *Carcinogenesis*, vol. 23, no. 3, pp. 425–434, 2002.
- [13] F. G. Bottone Jr., S. J. Baek, J. B. Nixon, and T. E. Eling, "Diallyl disulfide (DADS) induces the antitumorigenic NSAID-activated gene (NAG-1) by a p53-dependent mechanism in human colorectal HCT 116 cells," *Journal of Nutrition*, vol. 132, no. 4, pp. 773–778, 2002.
- [14] L. C. Wilson, S. J. Baek, A. Call, and T. E. Eling, "Nonsteroidal anti-inflammatory drug-activated gene (NAG-1) is induced by genistein through the expression of P53 in colorectal cancer cells," *International Journal of Cancer*, vol. 105, no. 6, pp. 747–753, 2003.
- [15] S. J. Baek, J.-S. Kim, F. R. Jackson, T. E. Eling, M. F. McEntee, and S.-H. Lee, "Epicatechin gallate-induced expression of NAG-1 is associated with growth inhibition and apoptosis in colon cancer cells," *Carcinogenesis*, vol. 25, no. 12, pp. 2425–2432, 2004.
- [16] J. B. Seung, J.-S. Kim, S. M. Moore, S.-H. Lee, J. Martinez, and T. E. Eling, "Cyclooxygenase inhibitors induce the expression of the tumor suppressor gene EGR-1, which results in the up-regulation of NAG-1, an antitumorigenic protein," *Molecular Pharmacology*, vol. 67, no. 2, pp. 356–364, 2005.
- [17] T. E. Eling, S. J. Baek, M. Shim, and C. H. Lee, "NSAID activated gene (NAG-1), a modulator of tumorigenesis," *Journal of Biochemistry and Molecular Biology*, vol. 39, no. 6, pp. 649–655, 2006.
- [18] T. Liu, A. R. Bauskin, J. Zaunder et al., "Macrophage inhibitory cytokine 1 reduces cell adhesion and induces apoptosis in prostate cancer cells," *Cancer Research*, vol. 63, no. 16, pp. 5034–5040, 2003.
- [19] Y.-L. Chen, P.-C. Lin, S.-P. Chen et al., "Activation of non-steroidal anti-inflammatory drug-activated gene-1 via extracellular signal-regulated kinase 1/2 mitogen-activated protein kinase revealed a isochaihulactone-triggered apoptotic pathway in human lung cancer A549 cells," *Journal of Pharmacology and Experimental Therapeutics*, vol. 323, no. 2, pp. 746–756, 2007.
- [20] T.-D. Way, J.-C. Lee, D.-H. Kuo et al., "Inhibition of epidermal growth factor receptor signaling by *Saussurea involucrata*, a rare traditional chinese medicinal herb, in human hormone-resistant prostate cancer PC-3 cells," *Journal of Agricultural and Food Chemistry*, vol. 58, no. 6, pp. 3356–3365, 2010.
- [21] L. K. Chao, P.-C. Liao, C.-L. Ho et al., "Anti-inflammatory bioactivities of honokiol through inhibition of protein kinase C, mitogen-activated protein kinase, and the NF- $\kappa$ B pathway to reduce LPS-induced TNF $\alpha$  and no expression," *Journal of Agricultural and Food Chemistry*, vol. 58, no. 6, pp. 3472–3478, 2010.
- [22] Y. C. Yang, H. Y. Lin, K. Y. Su et al., "Rutin, a flavonoid that is a main component of *Saussurea involucrata*, attenuates the senescence effect in D-galactose aging mouse model," *Evidence-Based Complementary and Alternative Medicine*, vol. 2012, Article ID 980276, 10 pages, 2012.
- [23] M. Chulasiri, N. Bunyapraphatsara, and P. Moongkarndi, "Mutagenicity and antimutagenicity of hispidulin and hortensin, the flavonoids from *Millingtonia hortensis* L," *Environmental and Molecular Mutagenesis*, vol. 20, no. 4, pp. 307–312, 1992.
- [24] B. Gil, M. J. Sanz, M. C. Ferrándiz et al., "Accelerated communication: effects of flavonoids on *Naja naja* and human recombinant synovial phospholipases A2 and inflammatory responses in mice," *Life Sciences*, vol. 54, no. 20, pp. PL333–PL338, 1994.
- [25] R. X. Tan, H. Lu, J.-L. Wolfender et al., "Mono- and sesquiterpenes and antifungal constituents from *Artemisia* species," *Planta Medica*, vol. 65, no. 1, pp. 64–67, 1999.
- [26] D. Kavvadias, V. Monschein, P. Sand, P. Riederer, and P. Schreier, "Constituents of sage (*Salvia officinalis*) with in vitro affinity to human brain benzodiazepine receptor," *Planta Medica*, vol. 69, no. 2, pp. 113–117, 2003.
- [27] D. Kavvadias, P. Sand, K. A. Youdim et al., "The flavone hispidulin, a benzodiazepine receptor ligand with positive allosteric properties, traverses the blood-brain barrier and exhibits anticonvulsive effects," *British Journal of Pharmacology*, vol. 142, no. 5, pp. 811–820, 2004.
- [28] Y.-C. Lin, C.-M. Hung, J.-C. Tsai et al., "Hispidulin potently inhibits human glioblastoma multiforme cells through activation of AMP-activated protein kinase (AMPK)," *Journal of Agricultural and Food Chemistry*, vol. 58, no. 17, pp. 9511–9517, 2010.
- [29] G. Mickisch, S. Fajta, G. Keilhauer, E. Schlick, R. Tschada, and P. A lken, "Chemosensitivity testing of primary human renal cell carcinoma by a tetrazolium based microculture assay (MTT)," *Urological Research*, vol. 18, no. 2, pp. 131–136, 1990.
- [30] M. van Engeland, L. J. Nieland, F. C. Ramaekers, B. Schutte, and C. P. Reutelingsperger, "Annexin V-affinity assay: a review on an apoptosis detection system based on phosphatidylserine exposure," *Cytometry*, vol. 31, no. 1, pp. 1–9, 1998.

- [31] L. F. Alfonso, K. S. Srivenugopal, T. V. Arumugam, T. J. Abbruscato, J. A. Weidanz, and G. J. Bhat, "Aspirin inhibits camptothecin-induced p21CIP1 levels and potentiates apoptosis in human breast cancer cells," *International Journal of Oncology*, vol. 34, no. 3, pp. 597–608, 2009.
- [32] F. V. Din, A. Valanciute, V. P. Houde et al., "Aspirin inhibits mTOR signaling, activates AMP-activated protein kinase, and induces autophagy in colorectal cancer cells," *Gastroenterology*, vol. 142, no. 7, pp. 1504–1515, 2012.
- [33] N. Wald, J. Morris, and M. Law, "Aspirin in the prevention of cancer," *The Lancet*, vol. 377, no. 9778, p. 1649, 2011.
- [34] A. V. Joshua, S. K. Sharma, A. Strelkov et al., "Synthesis and biodistribution of 8-iodo-11-(4-methylpiperazino)-5H-dibenzo[b,e][1,4]-diazepine: Iozapine," *Bioorganic and Medicinal Chemistry Letters*, vol. 17, no. 14, pp. 4066–4069, 2007.
- [35] K. Yamaguchi, S.-H. Lee, T. E. Eling, and S. J. Baek, "A novel peroxisome proliferator-activated receptor  $\gamma$  ligand, MCC-555, induces apoptosis via post-transcriptional regulation of NAG-1 in colorectal cancer cells," *Molecular Cancer Therapeutics*, vol. 5, no. 5, pp. 1352–1361, 2006.
- [36] S.-H. Lee, J.-S. Kim, K. Yamaguchi, T. E. Eling, and S. J. Baek, "Indole-3-carbinol and 3,3'-diindolylmethane induce expression of NAG-1 in a p53-independent manner," *Biochemical and Biophysical Research Communications*, vol. 328, no. 1, pp. 63–69, 2005.
- [37] D. Newman, M. Sakaue, J. S. Koo et al., "Differential regulation of nonsteroidal anti-inflammatory drug-activated gene in normal human tracheobronchial epithelial and lung carcinoma cells by retinoids," *Molecular Pharmacology*, vol. 63, no. 3, pp. 557–564, 2003.
- [38] P. A. Baeuerle, "I $\kappa$ B-NF- $\kappa$ B structures: at the interface of inflammation control," *Cell*, vol. 95, no. 6, pp. 729–731, 1998.
- [39] P.-C. Liao, S.-C. Chien, C.-L. Ho et al., "Osthole regulates inflammatory mediator expression through modulating NF- $\kappa$ B, mitogen-activated protein kinases, protein kinase C, and reactive oxygen species," *Journal of Agricultural and Food Chemistry*, vol. 58, no. 19, pp. 10445–10451, 2010.





# Hindawi

Submit your manuscripts at  
<http://www.hindawi.com>

